J Mol Model (2008) 14:1147–1157
DOI 10.1007/s00894-008-0357-1

ORIGINAL PAPER

Structural and dynamical studies of all-trans and all-cis cyclo[(1R,3S)-γ-Acc-Gly]$_3$ peptides

Gopalan Praveena · Ponmalai Kolandaivel

Received: 27 December 2007 / Accepted: 23 July 2008 / Published online: 16 September 2008

Abstract The quantum chemical and molecular dynamics studies have been performed to infer the structural changes of all-trans and all-cis forms of cyclo[(1R,3S)-3-aminocyclohexanecarboxylicacid(γ-Acc)-α-Glycine(Gly)]$_3$ hexapeptide. The backbone conformations of the above peptide have been analyzed using the valence and peptide deformation angles applying B3LYP/6–311G** level of theory. The conformational preference of the backbone of all-trans and all-cis cyclo[(1R,3S)-γ-Acc-Gly]$_3$ hexapeptides is found to depend on the puckering of cyclohexane rings. The non-uniform distribution of water inside the cavity is observed, where sometimes water molecules formed a chain like conformation through hydrogen bond networks while traversing the pore of all-cis cyclo[(1R,3S)-γ-Acc-Gly]$_3$ peptide. Larger relaxation times of the order of a hundred to two hundred pico seconds for active site… water hydrogen bond interactions were noticed. The hydrophobic nature of the cavity of all-trans cyclo [(1R,3S)-γ-Acc-Gly]$_3$ due to the presence of cyclohexane moiety has been analyzed. Further this investigation emphasized on the non-transport of molecules through the pore of all-trans cyclo[(1R,3S)-γ-Acc-Gly]$_3$ peptide due to the obstruction produced by cyclohexane groups.

Keywords α-γ cyclic peptides · Hydrogen bond dynamics · Hydrophobicity · Molecular dynamics simulations · Water transport

G. Praveena · P. Kolandaivel (✉)
Department of Physics, Bharathiar University,
641 046 Coimbatore, India
e-mail: ponkvel@hotmail.com

Introduction

Peptide based nanotubular arrays have been the subject of intense studies due to their possible efficacy in the field of organic/inorganic chemistry and in biomaterials. They were prepared by stacking of disk shaped or toroidal shaped cyclic peptide subunits through highly convergent non-covalent processes. It was De Santis et al., in 1974 [1] who first predicted the existence of cylindrical structures formed by β-type rings stacked either parallel or antiparallel and stabilized by means of backbone-backbone hydrogen bonding network. The initial attempts to verify this prediction were inconclusive [2, 3], and the first compelling evidence of nanotube formation by ring stacking of the cyclic peptide composed of [L-Glutamine(Gln)-D-Alanine (Ala)-L-Glutamicacid(Glu)-D-Alanine(Ala)]$_2$ units was made by Gadhri et al. [4]. Following this, considerable efforts have been made to synthesize the hollow tubular structures composed of various cyclic D, L-α [5–13], and β [14, 15] peptides. Later a new class of self-assembling nanotubular arrays based on the hybrid α-γ cyclic peptides has emerged [16–20]. All these synthetic cyclic peptides have augmented the potential utility of self-assembling peptide nanotubes and in particular, they have proven useful in the design of solid state porous materials [21], biologically relevant ion channels and pore assemblies [22–26]. In addition, the larger band gaps of these peptide nanotubes emphasize their use in the field of nanoelectronics and in other material science applications [27].

The most important characteristic of synthetic channel is its permeation properties, allowing water molecules to flow inside the pore. The charged sites and hydrophobicity are some of the factors, which play an important role in determining the rigidity of water molecules around the specific regions of peptides. Hence, the nature of interaction

between water and synthetic channels in aqueous solution is an important issue, to be discussed. There are studies concerning the analysis of water molecules inside the pore structures of D,L-α- cyclic peptides [10, 23, 24] and other naturally occurring channel forming tubules [28]. The dynamics of water molecules inside the tubular aquaporin-1 channel carried out by De Groot and Grubmüller [28] revealed the existence of fluctuating water column with temporary flouting behavior. There are assorted studies [4–26] that have demonstrated the channel properties of cyclic peptides, but understanding their infiltration properties toward water molecules at a microscopic level is still far from being complete.

Amorin et al. [20] have experimentally characterized the all-trans form of cyclo[(1R,3S)-γ-aminocyclohexanecarboxylicacid (Acc)-D-Aminoacid]$_3$ hexapeptide and its dimers by using nuclear magnetic resonance (NMR), Fourier transform infrared spectroscopy (FTIR) and X-ray crystallography. Distinct from the existing hydrophilic nanotubes [4–13], these novel peptides are found to have a functionalized hydrophobic inner cavity and have the ability to orient as self assembling peptide nanotubes. Also they are expected to have a greater selectivity toward the storage of molecules, ion channels and receptors [20]. Considering the importance of this new class of cyclic peptide systems toward the usage as molecular containers, we have performed quantum chemical and dynamic studies to understand their structural propensities and water transport behavior. For this, we have used the cyclo [(1R,3S)-γ-Acc-D-aminoacid]$_3$ hexapeptide model that consist of alternating (1R,3S)-γ-Acc and α-Glycine (Gly) subunits. The combined experimental and theoretical study [29] on heterochiral β-peptide sequences with alternating backbone configurations has indicated that all possible secondary structures of β-peptides can be made under stereochemical control. Hence the impact of stereomerism on the structural preference of cyclo[(1R,3S)-γ-Acc-Gly]$_3$ peptide should also be an important factor, which has to be analyzed. For this, we have constructed the all-trans and all-cis forms of cyclo[(1R,3S)-γ-Acc-Gly]$_3$ hexapeptide. The detailed comparative study on the structural preferences of both the peptides has been made through valence and peptide deformation angles. To our knowledge, this is the first theoretical study concerning the structural properties of the hybrids of α-γ self-assembling cyclic peptide systems.

It has been found experimentally that the symmetry of monohydrated pore of the cyclic hexapeptide consisting of alternating L-Proline and 3-aminobenzoic acid subunits is highly disturbed by the presence of a single water molecule, which in turn weakens the cationic affinity of the peptide [30]. Hence it emphasizes that study on the single pore of cyclic peptides would have theoretical and practical importance, which in turn would be helpful to understand the effect of guest molecules at the surface cavities of nanochannels. Here, we have carried out molecular dynamics (MD) simulations on the structures of all-trans and all-cis cyclo[(1R,3S)-γ-Acc-Gly]$_3$ hexapeptides obtained by density functional theory (DFT) optimizations to understand their dynamical and water transport aspects. The behavior of water molecules in the vicinity of cyclic peptides and their life time around the active sites have been examined through hydrogen bond dynamics.

System construction and computations

The all-trans form of cyclo[(1R,3S)-γ-Acc-Gly]$_3$ hexapeptide is optimized using DFT method applying hybrid exchange-correlation functional named B3LYP (Becke'3 parameter for the exchange and Lee, Yang and Parr for the electronic correlation) [31–33]. The main chain atoms of this cyclic peptide with trans -NH-CO- peptide bond lie in the same plane, with C=O and N-H groups lying roughly perpendicular to the plane of the peptide. The -NH-CO- group with cis geometry, another vital conformation in lactams, is found to take part in proteins to form lactam bridges [34]. An attempt has also been made to construct the all-cis form of cyclo[(1R,3S)-γ-Acc-Gly]$_3$. The basis set with polarization function 6–311G** [35–37] has been used for optimizations. Both the peptides were modeled using Molden software [38] and all the calculations were carried out using Gaussian 98W program package [39].

The puckering of six membered rings present in all-trans and all-cis cyclo[(1R,3S)-γ-Acc-Gly]$_3$ hexapeptides has been analyzed and compared. The exact definition of three puckering coordinates for the six-membered ring was first reported by Cremer and Pople [40]. Because of the inconsistency in their formalism [41], an alternative conformational analysis has been facilitated by truncated Fourier (TF) formalism [42], which describes the interdependence of six endocyclic torsions (ϕ_j, j=0,…5, cf in Fig. 1) viz.,

$$\phi_j = \Phi_2 \cos\left(P_2 + 4\pi_j/6\right) + \Phi_3 \cos\left(\pi_j\right) \quad (1)$$

where Φ_2, Φ_3, and P_2 are the puckering coordinates that were replaced by a spherical polar set (P_2, θ, Q) as,

$$Q = \sqrt{\Phi_2^2 + \Phi_3^2} \quad (2)$$

$$\theta = \arctan(\Phi_2/\Phi_3) \quad (3)$$

where Q is the puckering amplitude with $0 \leq \theta \leq \pi$ [42].

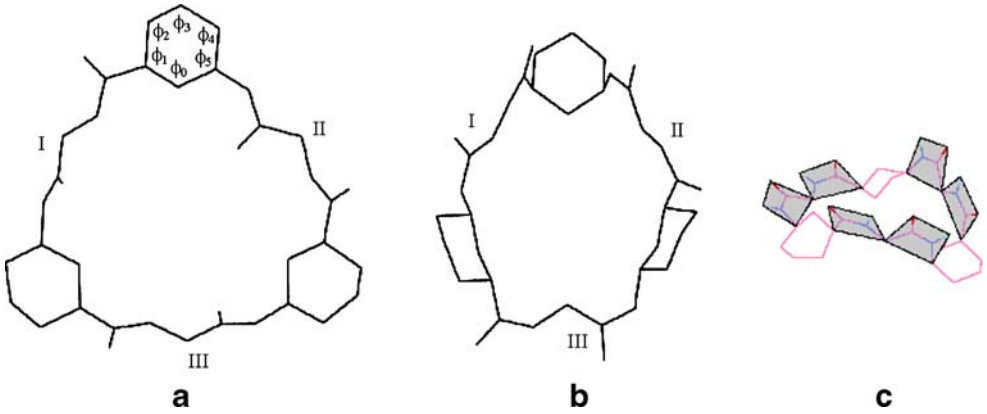

Fig. 1 Optimized structures of a) all-trans and b) all-cis of cyclo[(1R,3S)-γ-Acc-Gly]$_3$ hexapeptides (with six-membered ring endocyclic torsional angles ϕ_0, ϕ_1, ϕ_2, ϕ_3, ϕ_4 and ϕ_5) and c) Representation of all-cis cyclo[(1R,3S)-γ-Acc-Gly]$_3$ plaques

Simulation

The possible disadvantage of quantum chemical calculations would be the non-predictability of multiple minima in the energy surface of larger molecules [43, 44]. Since the systems that we have considered in the present study are having greater number of atoms, it is very difficult to identify the global minima using density functional method. Further, we have also tried to change some of the peptide deformation angles like ω_1, ω_2, ω_3, etc., (shown in Fig. 2) to perform optimization. However, while altering the peptide deformation angles from one to another, the cyclicity of the peptide breaks. Though multiple minima problem for finding the global minimum energy conformation of a large system persists, one of the approaches which have been proposed in response to the challenge of solving the multiple minima problem is a molecular dynamics simulation [44–46]. We have simulated the all-trans and all-cis forms of cyclo [(1R,3S)-γ-Acc-Gly]$_3$ hexapeptides in vacuum at room temperature for over 1 ns to examine their energy surface. We have observed that the distribution of peptide deformation angles ω_1, ω_2, ω_3, ω_4, ω_5 and ω_6 accounts for maximum probability around 0 to 10° for all-cis cyclo[(1R,3S)-γ-Acc-Gly]$_3$ hexapeptide (see in Fig. 3a). And for all-trans peptide, the maximum probability of ω angles lies in the range of -180 to -170° approximately (Fig. 3b). This agrees with the deformation angles obtained by DFT optimization for both the peptides (given in Table 1). Hence, from this we came to the conclusion that the optimized structures of all-trans and all-cis cyclo[(1R,3S)-γ-Acc-Gly]$_3$ hexapeptides obtained by DFT would be the global minima.

The duly optimized structures of all-trans and all-cis cyclo[(1R,3S)-γ-Acc-Gly]$_3$ hexapeptides were then subjected to large scale atomistic MD simulations in explicit water. The systems were examined with constant pressure periodic boundary condition, wherein the Langevin piston maintained the pressure of the cell at 1 atm. The information of both the systems prepared up for simulation

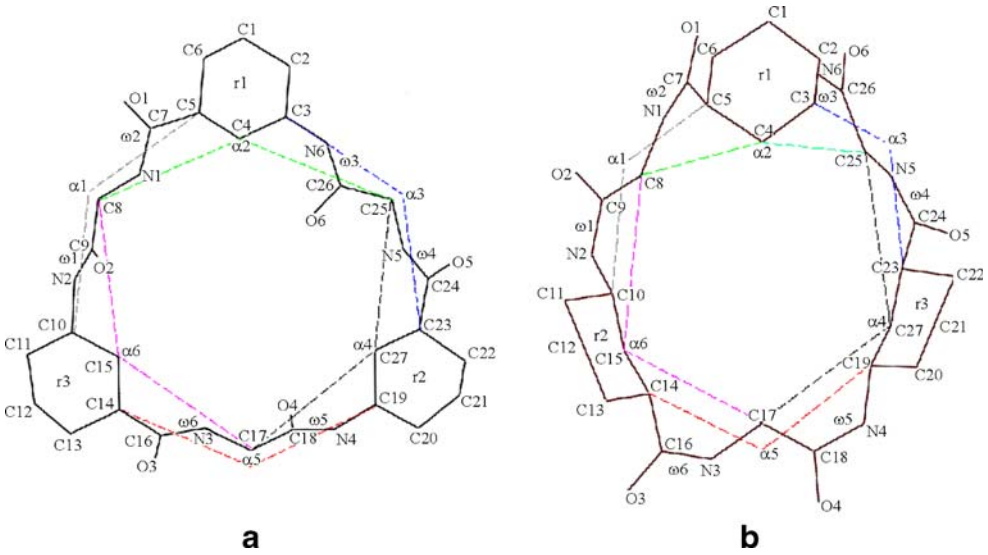

Fig. 2 Illustration of valence angles (α_1, α_2, α_3, α_4, α_5 and α_6) and deformation angles ω_1 - C8-C9-N2-C10, ω_2 - C5-C7-N1-C8, ω_3 - C25-C26-N6-C3, ω_4 - C23-C24-N5-C25, ω_5 - C17-C18-N4-C19, ω_6 - C14-C16-N3-C17 of a) all-trans and b) all-cis cyclo [(1R,3S)-γ-Acc-Gly]$_3$ hexapeptides. Numbering scheme depicted in the picture is followed through out the study

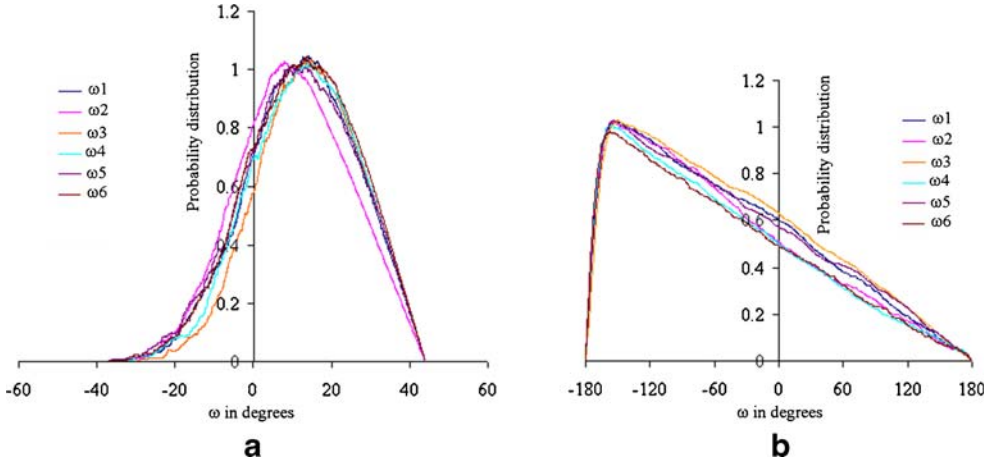

Fig. 3 Probability distribution of peptide deformation angles of a) all-cis and b) all-trans cyclo[(1R,3S)-γ-Acc-Gly]$_3$ hexapeptides simulated in vacuum for 1 ns at 300 K

is given in Table 2. The Langevin dynamics was used to control the temperature at 300K with the collision frequency of 1.5 ps^{-1}. Bonds involving hydrogen atoms were constrained to their equilibrium value by means of SHAKE algorithm. The non-bonded cut off distance of 10.0Å is employed for simulation. Hornak et al [47] have compared the multiple Amber force fields for the protein backbone parameters and found that ff03 force field fits better with the experimental data than other force fields. Hence we have used ff03 force field [48] to extract the torsional and non-bonded energy parameters of both the cyclic peptides. As TIP3P water model [49] is found to be well balanced [50] with Amber force field, it is used here for water modeling. The simulation was carried out for over 10 ns duration with a MD time step of 2 fs. All the simulations presented here were carried out using the program AMBER version 8.0 [51].

Results and discussion

Structural description of all-trans and all- cis cyclic peptides

This section explores the preliminary structural parameters to understand the molecular arrangements of all-trans and all-cis cyclo[(1R,3S)-γ-Acc-Gly]$_3$ hexapeptides. Figure 1(a,b) shows the optimized structure of the peptides, wherein their sides were grouped as I, II and III. The backbone conformations of all-trans cyclo[(1R,3S)-γ-Acc-Gly]$_3$ is essentially flat with C=O and N-H groups lying roughly perpendicular to the plane of the peptide (given in Fig. 1a). Plaque, the mean plane associated with six atoms $C_\alpha C'ONHC_\alpha$ that participate in the cis peptide bond as shown in Fig. 1c, is the best tool to explain the conformation of all-cis cyclic peptides [52]. The arrangement of plaques in all-cis cyclo[(1R,3S)-γ-Acc-Gly]$_3$ shows that the peptide adopts a vessel-like structure. The plaques at sides I and II are tilted upwards from the plane of the peptide, while at side III, it is coplanar with the peptidic plane. Hence, the overall shape of all-cis peptide is found to be a constrained planar symmetry with plaques and part of cyclohexane groups facing outside.

An important parameter that describes the structural arrangement of plaques in all-cis α-cyclic peptides is the valence angle α between C_α carbon atoms [52] shown in Fig. 2. We have made use of valence angles (α_1, α_2, α_3, α_4, α_5 and α_6) and also the peptide deformation angles (ω_1, ω_2, ω_3, ω_4, ω_5 and ω_6) given in Table 1 to infer the backbone conformation of both the all-trans and all-cis cyclo[(1R,3S)-γ-Acc-Gly]$_3$ hexapeptides. These angles are found to coincide well with the previously reported values for cyclic peptides [52]. A closer look at the α angles of all-trans cyclo[(1R,3S)-γ-Acc-Gly]$_3$ tilts around 135–138°, which confers to the extended backbone conformation. Because of the stumbling arrangement of plaques, the distortion is spread over the backbone of all-cis cyclo[(1R,3S)-γ-Acc-

Table 1 Valence angles α_1, α_2, α_3, α_4, α_5 and α_6 (in degrees), deformation angles ω_1, ω_2, ω_3, ω_4, ω_5 and ω_6 (in degrees) and total energy (in hartrees) of all-trans and all-cis cyclo[(1R,3S)-γ-Acc-Gly]$_3$ hexapeptides at B3LYP/6–311G** level of theory

System	α_1	α_2	α_3	α_4	α_5	α_6	ω_1	ω_2	ω_3	ω_4	ω_5	ω_6	Total Energy
Trans	136.1	137.6	136.4	137.7	135.9	137.9	170.4	-179.6	170.4	179.9	170.0	-179.6	-1834.644
Cis	138.5	104.2	132.2	117.5	137.9	120.3	7.9	0.9	0.0	0.1	5.1	3.6	-1834.614

Note: the valence angles α1, α2, α3, α4, α5 and deformation angles ω1, ω2, ω3, ω4, ω5 and ω6 are depicted in Fig. 2

Table 2 Simulation set-up prepared to run molecular dynamics for all-trans and all-cis cyclo[(1R,3S)-γ-Acc-Gly]$_3$ hexapeptides

Solute	Force field	No. of water molecules	Volume of the simulation box Å3	Solvent	Simulation length (ns)	Temperature (K)	Dimension of the PBC box Å3
Trans	Leaprcff03	1009	47203.6	H_2O	10	300	39.6×40.3×29.6
Cis		1027	47173.6				39.6×37.8×31.6

Gly]$_3$, which is reflected in the reduction of α_2, α_3 and α_5 angles from 135° to 100° approximately. As a consequence, unlike flat shaped all-trans cyclic peptide, the backbone conformation of all-cis cyclic peptide is disturbed and takes a non-planar conformation adopting a vessel like structure as previously found for various all-cis cyclopeptides [52].

Further the considered cyclic peptide systems contain cyclohexane groups with their β-methylene moiety inside the cavity as shown in Fig. 1. Such cyclohexane groups may play an important role in deciding the preferential conformation of the backbone of cyclic peptides. The interrelation between the six-membered rings and the backbone conformation is analyzed by the use of puckering coordinates. The conformational accessibility of the six-membered rings is possible using the puckering coordinates P_2, θ and Q [42]. Every six-membered ring conformation may be viewed in terms of boat (B), twist-boat (T), chair (C), half chair (H) and envelope (E) [42]. If for a given system all the endocyclic angles ϕ_0, ϕ_1, ϕ_2, ϕ_3, ϕ_4 and ϕ_5 as given in Fig. 1a are known, then the puckering coordinates can be calculated with the aid of Eqs. 1, 2 and 3. The puckering coordinates of six-membered rings r_1, r_2 and r_3 (Fig. 2) of the all-trans and all-cis cyclo[(1R,3S)-γ-Acc-Gly]$_3$ hexapeptides are calculated and tabulated in Table 3.

The rings of all-trans cyclo[(1R,3S)-γ-Acc-Gly]$_3$ are found to be characterized by P_2=~135°-137°, θ=~93° and Q=~36°, which are fixed to T conformation [42]. In all-cis cyclic peptide, analysis of the puckering coordinates imply that the rings r_1 and r_2 adopt chair and boat conformations, while the ring r_3 takes up T conformation with P_2=140.9°, θ=36.9° and Q=92.7°. The rings r_1 and r_2 have taken up the C and B conformations due to the distortion in ω_2 and ω_3 angles (7.94° and 3.58°) from the normal 0° cis peptide plane angle. This buckling along the backbone at sides I and II in turn may be the outcome of plaques upward twist which is indicated in Fig. 1c. Overall, it is found that the conformation of six-membered rings correlate well with the structural distribution of the backbone of cyclo[(1R,3S)-γ-Acc-Gly]$_3$ hexapeptides.

Further the calculated total energies of all-trans and all-cis cyclo[(1R,3S)-γ-Acc-Gly]$_3$ hexapeptides listed in Table 1 shows a larger energy barrier of about 18.8 kcal mol^{-1} between the cyclic peptides. The van der Waals inner diameter and cavity height of all-trans and all-cis cyclic peptides are also given in Table 4. The single pore diameter of all-trans cyclo[(1R,3S)-γ-Acc-Gly]$_3$ peptide is found to be larger than that of the cyclo[(1R,3S)-γ-Acc-Ala]$_3$ dimers [20]. The reason may be the greater flexibility of peptide backbone, which may not sample rings with larger diameters due to entropic effects in the flat ring shaped conformational state [21].

Behavior of all-trans and all-cis cyclo[(1R,3S)-γ-Acc-Gly]$_3$ hexapeptides

A complete analysis of all-trans and all-cis cyclo[(1R,3S)-γ-Acc-Gly]$_3$ hexapeptides embedded in water is carried out using MD simulations for over 10 ns. From the time evolution of the diameter in Fig. 4a, it is clear that the dimension of all-cis cyclic peptide is well conserved with

Table 3 Endocyclic torsion angles (ϕ_0, ϕ_1, ϕ_2, ϕ_3, ϕ_4 and ϕ_5) (in degrees), pseudo-rotational parameters Φ_2, Φ_3, P_2, Q and θ (in degrees), and conformations (T- Twist boat; B- Boat and C- Chair) of the six-membered rings present in all-trans and all-cis cyclo[(1R,3S)-γ-Acc-Gly]$_3$ hexapeptides obtained at B3LYP/6–311G** level of theory

System	ϕ0	ϕ1	ϕ2	ϕ3	ϕ4	ϕ5	Φ2	Φ3	P2	Q	θ	Conformation*
Trans												
I	-27.9	-33.0	61.2	-23.9	-36.7	65.1	36.2	-1.9	137.6	36.2	93.1	T
II	-27.4	-33.5	60.8	-22.9	-37.5	65.1	36.1	-2.1	135.9	36.2	93.4	T
III	-28.1	-32.8	61.1	-23.8	-36.9	65.3	36.3	-2.0	137.6	36.3	93.2	T
Cis												
I	-50.3	52.3	-53.7	53.6	-52.9	51.1	42.7	52.3	87.8	67.6	39.2	C
II	-30.8	61.7	-26.9	-33.6	64.7	-30.2	36.1	-1.5	156.3	36.1	92.4	B
III	-26.1	62.8	-32.6	-29.5	66.2	-35.9	36.8	-1.7	140.9	36.9	92.8	T

Table 4 Cavity diameter (in Å), height (in Å) and molecular volume (in cm^3/mol) of all-trans and all-cis cyclo[(1R,3S)-γ-Acc-Gly]$_3$ hexapeptides

System	Top rim	Cavity height	Molecular Volume
Trans	8.645	2.741	449.0
Cis	6.786	2.736	393.8

minimal distortion in its backbone. The original flat conformation of all-trans cyclo[(1R,3S)-γ-Acc-Gly]$_3$ is however modified within a moment of simulation forming a bowl like structure with cyclohexane groups at the concave side (Fig. 4d). This distortion in the backbone of all-trans peptide is also readily observed from the variation in the valence angles (Fig. 5(a,b)). The angles α_1, α_2, α_3, and α_4 (Fig. 5b) of all-trans cyclo[(1R,3S)-γ-Acc-Gly]$_3$ changes significantly from the extended conformation that has α value around 135°. To study the planarity of the peptides, time evolution of the angle (ζ) between atoms that are chosen randomly along the backbone is noted, which clearly shows (Fig. 5(e,f)) that all-trans peptide is highly distorted from the initial conformation during the time of simulation.

The initial and instantaneous trajectories of the peptides are given in Fig. 6. It is seen from the picture that during simulation, the all-trans and all-cis cyclo[(1R,3S)-γ-Acc-Gly]$_3$ hexapeptides involve in hydrogen bond interactions with the surrounding water molecules. In the following sections, these intermolecular hydrogen bond interactions can be examined with the help of hydrogen bond analysis, radial distribution functions and from the life time of active sites (O, N and C of Peptide)…water (Wat) assemblies.

Bonding facets of cyclo[(1R,3S)-γ-Acc-Gly]$_3$ active sites

The H-bond analysis of all-trans and all-cis cyclo[(1R,3S)-γ-Acc-Gly]$_3$ in water reveals that the oxygen (O), nitrogen (N) and carbon (C) atoms of the peptide backbone, actively take part in hydrogen bonds with water molecules as H-bond donors. The comparison between O(Peptide)…H(Wat) radial distribution functions (RDF) of the all-trans and all-cis cyclo[(1R,3S)-γ-Acc-Gly]$_3$ reveal that the coordination shells are characterized by a major peak around 1.7Å (Fig. 7(a,b)). At the minimum of 1.7Å, on average, only one water molecule constitutes the coordination shell of both peptides through out the simulation (Fig. 7c). However, the sharpness of the peaks at certain periods (say around 1.7, 2.25, 6.3, 7.5, 8 ns etc.,) seldom shows two/three water molecules can also occupy this shell. The next immediate coordination shell can be easily identified from O(Peptide)…H(Wat) RDFs with the peak featuring nearly unity at around 2.6Å (Fig. 7(a,b)), and the consequent number of water molecules within this solvation shell is depicted in Fig. 7d. The RDFs of O(Peptide)…O(Wat) and N(Peptide)…O(Wat) assemblies

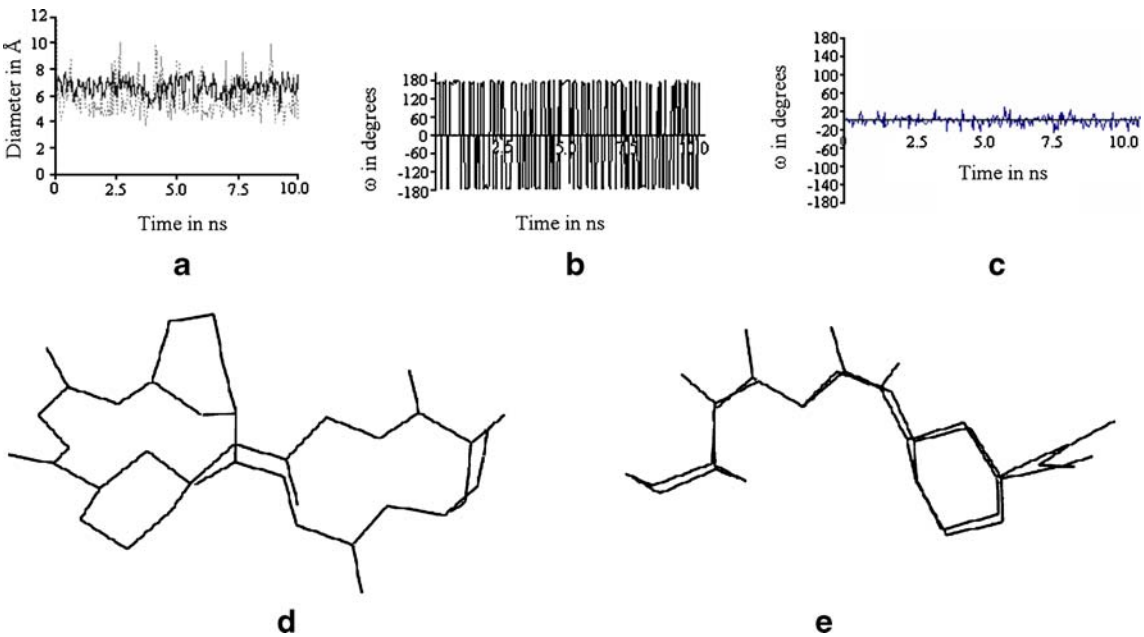

Fig. 4 a) Time progression of (a) diameter of all-cis (solid line) and all-trans (dashed lines). (b) Variation in the deformation angles of all-trans (c) Variation in the deformation angles of all-cis. Average backbone structure of (d) all-trans and (e) all-cis cyclo[(1R,3S)-γ-Acc-Gly]$_3$ hexapeptides

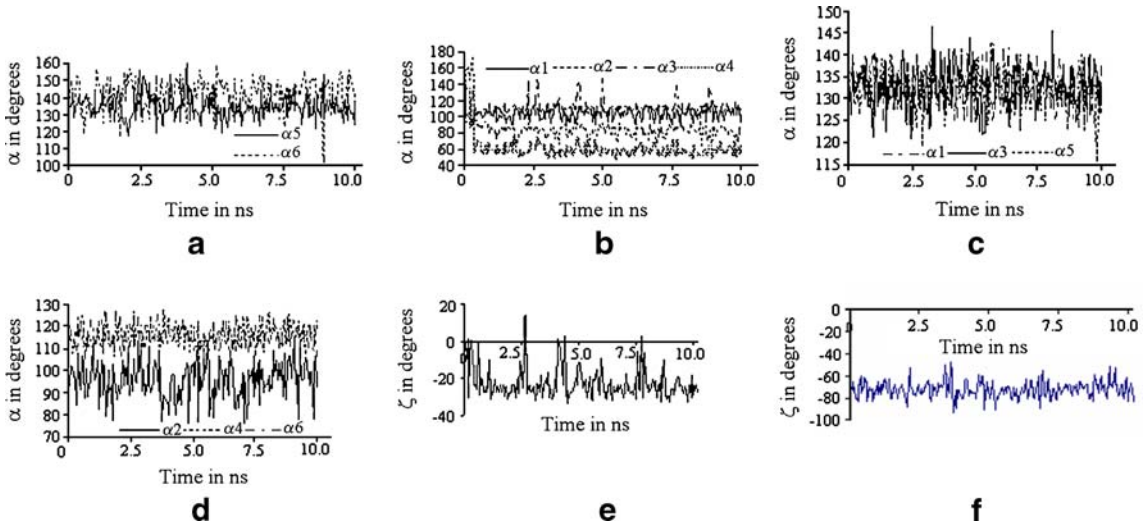

Fig. 5 Time progression of valence angles for all-trans structure: (a) α that takes ≥130˚ values and (b) that falls below 130˚. Time progression of valence angles for all-cis structure: (c) α that takes ≥130˚ values and d) α below 130˚. Variation in the planarity of e) all-trans and f) all-cis cyclo[(1R,3S)-γ-Acc-Gly]$_3$ hexapeptides

are also illustrated in Fig. 7(a,b). The O(Peptide)…O (Wat) distribution function approaches a maximum at quite larger distances of 2.6Å and is comparable in both the all-trans and all-cis cyclo[(1R,3S)-γ-Acc-Gly]$_3$ hexapeptides. These distribution functions are the indication of hydrogen bonds between acceptor of the solute and donors of water molecules, and are similar to the previously suggested results for hydroxide ion-water system [53].

Lifetimes of peptide…water hydrogen bond interactions

It is the basic feature that structural organization and dynamics of water molecules coupled to the molecular interface are highly dependent of inter-molecular hydrogen bond interactions [54–58]. Also the formation and breaking of such hydrogen bonds play an important role in determining the functionality of proteins. Either a geometric [54, 56, 59] or energetic [60, 61] criterion can be used to

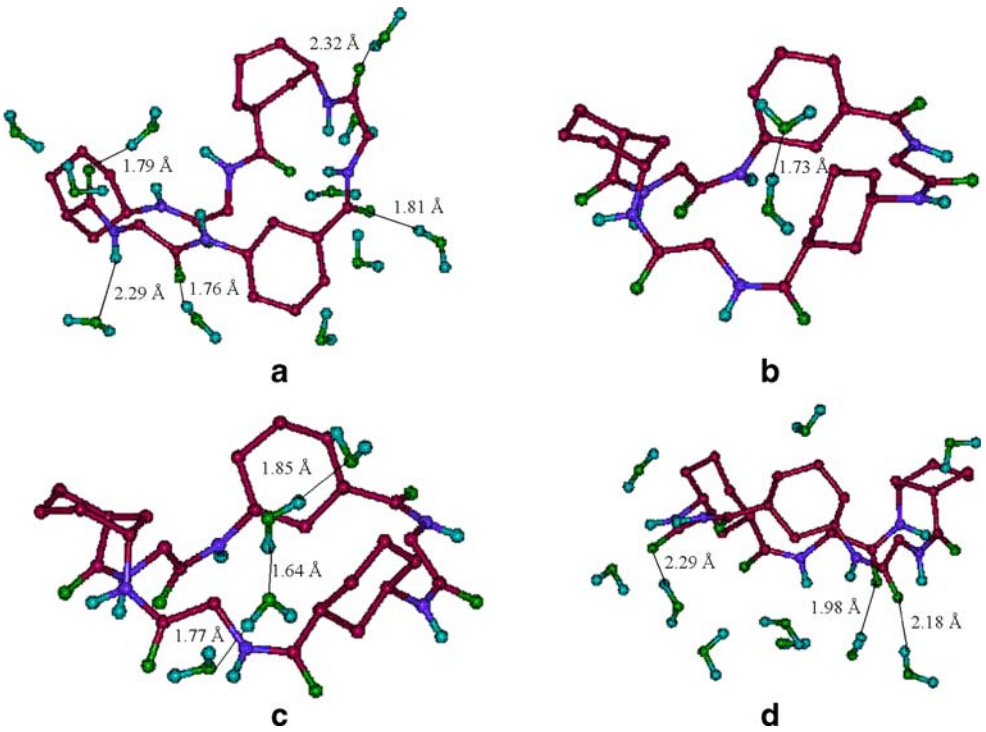

Fig. 6 Selected conformations showing the arrangement of water molecules (a) in all-trans and, (b, c and d) in all-cis cyclo [(1R,3S)-γ-Acc-Gly]$_3$ hexapeptides

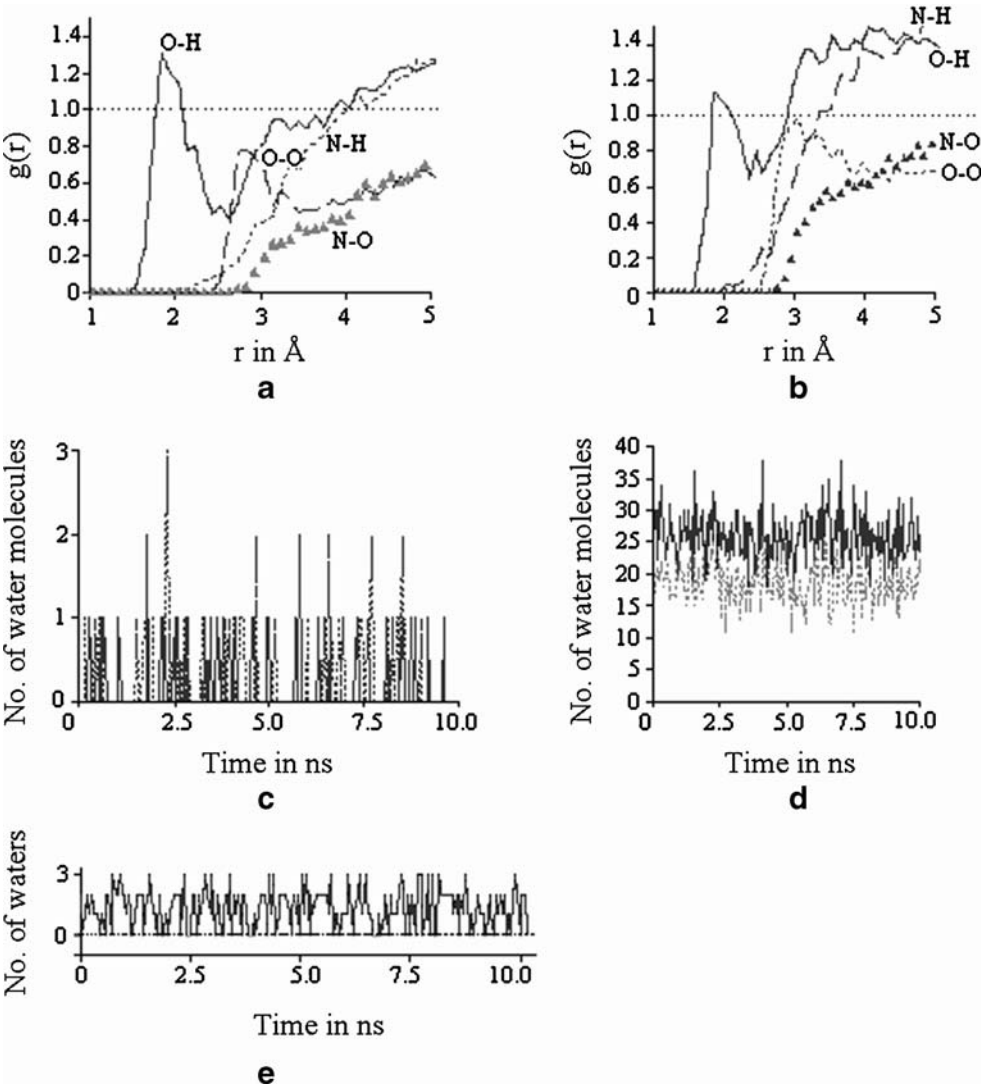

Fig. 7 Oxygen (Peptide)…Hydrogen (Wat), Oxygen (Peptide)…Oxygen (Wat), Nitrogen (Peptide)…Oxygen (Wat) and Nitrogen (Peptide)…Hydrogen (Wat) radial distribution functions of a) all-trans and b) all-cis cyclo [(1R,3S)-γ-Acc-Gly]$_3$ hexapeptides in water. Time progression of the number of water molecules in the shells of (c) 1.7Å and (d) 2.6Å. (e) Time evolution of number of water molecules getting inside the pore of all-trans and all-cis cyclo[(1R,3S)-γ-Acc-Gly]$_3$ hexapeptides. (Dotted lines represent all-trans and solid curves represent all-cis cyclic peptides)

describe the nature of hydrogen bonds. We report the structural relaxation of hydrogen bonds of the cyclo [(1R,3S)-γ-Acc-Gly]$_3$ peptide active site…Wat assemblies using time correlation function,

$$C(t) = \frac{\langle h(t+\tau).h(\tau)\rangle}{\langle h\rangle} \quad (4)$$

where hydrogen bond variable *h(t)* is unity when active site…water pair is bonded at time 't' according to the definition used or zero otherwise. The angular bracket denotes averaging over time and the correlation function *C (t)* describes the probability of particular active site…Wat hydrogen bond at time t.

Figure 8 shows the variation of *C(t)* against time for active site…Wat assemblies. It is clearly evident that the structural relaxation of O(Peptide)…Wat and N(Peptide)…Wat H-bonds are slower than the C(Peptide)…Wat interactions in both all-trans and all-cis cyclo[(1R,3S)-γ-Acc-Gly]$_3$ peptides. Further, the long time decay of the curves is an indication of the existence of slow components. Hence, we have used multiexponentials to fit such slow long time decay curves and obtained relaxation time τ for O, N and C…Wat hydrogen bond interactions [62-66]. Also we have utilized the sum of three exponentials to fit the correlation functions $C_{OW}(t)$ and $C_{NW}(t)$ of O(Peptide)…Wat and N (Peptide)…Wat interactions and two exponentials to fit the $C_{CW}(t)$ of C(Peptide)…Wat decay curves. The average relaxation times of O(Peptide)…Wat, N(Peptide)…Wat and C(Peptide)…Wat assemblies obtained from the fit are given in Table 5. It is noted that the life times of hydrogen bonds involving oxygen and nitrogen atoms are much larger than carbon life time. Such larger life times may be due to the

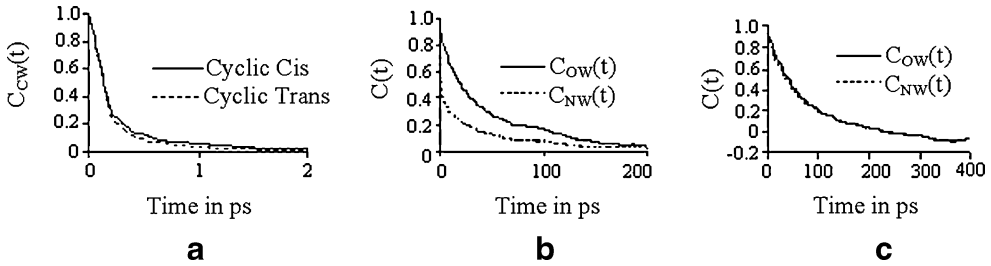

Fig. 8 Time correlation function (TCF) of active site…water assemblies a) TCF of C(Peptide)…Wat interactions in all-cis (Solid line) and all-trans (dotted lines) cyclic peptides. TCFs of O(Peptide)… Wat and N(Peptide)…Wat interactions in b) all-trans and c) all-cis cyclo[(1R,3S)-γ-Acc-Gly]$_3$ hexapeptides

slower mobility of water molecules near the polar/charged peptide active sites [67, 68].

Comportment and orientation of water molecules

During the run, spontaneous diffusion of water molecules inside the cavity of all-cis cyclo[(1R,3S)-γ-Acc-Gly]$_3$ is seen. However, the diffusion of water molecules through the pore of all-trans cyclo[(1R,3S)-γ-Acc-Gly]$_3$ is found to be absent. From the peptide-water molecular structural arrangement, this strange behavior of all-trans and all-cis cyclo[(1R,3S)-γ-Acc-Gly]$_3$ hexapeptides is discussed and compared.

Snapshots for all-cis cyclo[(1R,3S)-γ-Acc-Gly]$_3$ in Fig. 6(b,c,d) at different points along the trajectory shows a variety of peptide organizations. It is also seen that the water molecules form hydrogen bonds with peptides and within themselves during simulation. Also, the trajectories depict that water molecules may take diverse conformations through hydrogen bonded networks while passing through the pore. The number of water molecules getting inside the pore of all-cis cyclo[(1R,3S)-γ-Acc-Gly]$_3$ (Fig. 7e) during the course of simulation is found to be 3 with little fluctuations in their order (0–3 water molecules). This type of water fluctuations inside the cavity of peptide nanotubes were observed previously [23, 28]. Further, in most cases, the cavity height of all-cis channel is found to accommodate approximately three water molecules through intermolecular hydrogen bonding and such water molecules adopt a part of chain conformation as seen in Fig. 7c. The formation of such a water column inside the pores of nanotubular structures was also discussed by various groups [10, 13, 23, 28].

Table 5 Active site…water hydrogen bond relaxation time (τ) (in ps) of all-trans and all-cis cyclo[(1R,3S)-γ-Acc-Gly]$_3$ hexapeptides

Active site…Water	Relaxation time (τ)	
	Trans	Cis
O…WAT	129.2	261.4
N…WAT	57.2	296.0
C…WAT	0.32	0.41

During simulation, the configurations of the all-trans peptide have undergone a drastic change from the flat shaped initial conformation to a compressed curved cupel like structure as shown in Fig. 4d. The width of all-trans channel is well enough to accommodate three water molecules, but none of the water molecules were found to pass through its pore (Fig. 7e). Due to the buckling of hydrophobic cyclohexane groups, the methylene moiety blocks the cavity of all-trans peptide as shown in Fig. 4d. When the water molecules approach such a blocked pore, they would attain relatively higher mobility at the carbon sites of methylene groups, which is evident by the smaller life time of C(peptide)…Wat assemblies. Hence, the water molecules have not traversed the pore of all-trans peptide, thus escaping from the surface. Even though no directional flow of water molecules inside the pore of all-trans was observed, most of them were found to be present at the backbone, which further highlights the hydrophobic character of cyclohexane moiety. Such a behavior of all-trans cyclo[(1R,3S)-γ-Acc-Gly]$_3$ during simulation emphasize that the blockage of pore may prevent the channel of all-trans from interacting with other guest molecules.

In general, two structural arrangements of water molecules were found i) water molecules inside the cavity and ii) water molecules at the surface with none inside the pores (Fig. 6). It is clear from the snapshots that the distribution of water molecules is not uniform. The empty hydration domains with water molecules on the surface of peptides spanning hundreds of picoseconds are noted in Fig. 7e. This may be the sign of temporary splitting of water column inside the cavity as observed previously in the aquaporin-1 channel [28]. Generally, the all-cis cyclo [(1R,3S)-γ-Acc-Gly]$_3$ creates a center of attention drawing water molecules nearby and conducts them through its channel. The all-trans cyclo[(1R,3S)-γ-Acc-Gly]$_3$ pore is highly hydrophobic toward approaching water molecules, a

behavior due to structural distortion by its methylene moiety depicting their functionalized nature.

Concluding remarks

The quantum chemical calculations on the structural preferences of all-trans and all-cis cyclo[(1R,3S)-γ-Acc-Gly]$_3$ hexapeptides emphasize the conformational dependence of backbone with the puckering of cyclohexane rings. A good structural agreement for all-trans structure is found with the previously obtained configurations. In-depth analysis of the trajectory shows that both all-trans and all-cis cyclo[(1R,3S)-γ-Acc-Gly]$_3$ hexapeptides sustain their configuration rigidly throughout the simulation. However, a major disruption at the initial stage is observed for all-trans cyclic peptide. During the course of simulation, it is found that the cavity of all-cis cyclo[(1R,3S)-γ-Acc-Gly]$_3$ is able to conduct water molecules in a much better fashion than all-trans pore. Hence all-cis cyclo[(1R,3S)-γ-Acc-Gly]$_3$ channel is suitable for various ions and molecular transport. The non-conductance of water molecules through all-trans cyclic peptide pore shows that overall conductance depends on the alignment of the cyclohexane groups. As a consequence, all-trans peptide channel may not act as a molecular container unless the cyclohexane moiety is locked.

Acknowledgements The authors are thankful to the Council of Scientific and Industrial Research (CSIR), India for awarding the project (Project No: 03(1051)/06 EMR II).

References

1. De Santis P, Morosetti S, Rizzo R (1974) Macromolecules 7:52–58
2. Tomasic L, Lorenzi GP (1978) Helv Chim Acta 70:1012–1016
3. Pavone V, Benedetti E, Di Blasco B, Lombarda A, Pedone C, Tomasic L, Lorenzi GP (1989) Biopolymers 28:215–223
4. Ghadiri MR, Granja JR, Milligan RA, McRee DE, Khazanovich N (1993) Nature 366:324–327
5. Khazanovich N, Granja JR, McRee DE, Milligan RA, Ghadiri MR (1994) J Am Chem Soc 116:6011–6012
6. Ghadiri MR, Granja JR, Buehler LK (1994) Nature 369:301–304
7. Ghadiri MR (1995) Adv Mater 7:675–677
8. Lewis JP, Pawley NH, Sankey OF (1997) J Phys Chem B 101:10576–10583
9. Kim HS, Hartgerink JD, Ghadiri MR (1998) J Am Chem Soc 120:4417–4424
10. Tarek M, Maigret B, Chipot C (2003) Biophys J 85:2287–2298
11. Khurana E, Nielsen SO, Ensing B, Klein ML (2006) J. Phys Chem B 110:18965–18972
12. De Santis P, Morosetti S, Scipioni A (2007) J Nanosci Nanotechnol 7:2230–2238
13. Chipot C, Tarek M (2006) Phys Biol 3:S20–S25
14. Seebach D, Matthews JL, Meden A, Wessels T, Baerlocher C, McCusker LB (1997) Helv Chim Acta 80:173–182
15. Clark TD, Buehler LK, Ghadiri MR (1998) J Am Chem Soc 120:651–656
16. Kubik S, Goddard R (1999) J Org Chem 64:9475–9486
17. Kubik S (1999) J Am Chem Soc 121:5846–5855
18. Pohl S, Goddard R, Kubik S (2001) Tetrahedron Lett 42:7555–7558
19. Ishida H, Qi Z, Sokabe M, Donowaki K, Inoue Y (2001) J Org Chem 66:2978–2989
20. Amorin M, Castedo L, Granja JR (2003) J Am Chem Soc 125:2844–2845
21. Hartgerink JD, Granja JR, Milligan RA, Ghadiri MR (1996) J Am Chem Soc 118:43–50
22. Granja JR, Ghadiri MR (1994) J Am Chem Soc 116:10785–10786
23. Engles M, Bashford D, Ghadiri MR (1995) J Am Chem Soc 117:9151–9158
24. Asthagiri D, Bashford D (2002) Biophys J 82:1176–1189
25. Dehez F, Tarek M, Chipot C (2007) J Phys Chem B 111:10633–10635
26. Ferrante F, La Manna G (2007) J Comput Chem 28:2085–2090
27. Praveena G, Kolandaivel P, Santhanamoorthi N, Renugopalakrishnan V, Ramakrishna S (2007) J Nanosci Nanotechnol 7:2253–2259
28. De Groot BL, Grubmüller H (2001) Science 294:2353–2357
29. Martinek TA, Mándity IM, Fülöp L, To'th GK, Vass E, Hollósi M, Forró E, Fülöp F (2006) J Am Chem Soc 128:13539–13544
30. Kubik S, Goddard R (2000) Chem Commun :633–634
31. Lee C, Yang W, Parr RG (1988) Phys Rev B 37:785–789
32. Miehlich B, Savin A, Stoll H, Preuss H (1989) Chem Phys Lett 157:200–206
33. Becke ADJ (1993) J Chem Phys 98:5648–5652
34. Taylor JW (2002) Biopolymers 66:49–75
35. McLean AD, Chandler GS (1980) J Chem Phys 72:5639–5648
36. Krishnan R, Binkley JS, Seeger R, Pople JA (1980) J Chem Phys 72:650–654
37. Frisch MJ, Pople JA, Binkley JS (1984) J Chem Phys 80:3265–3269
38. Schaftenaar G, Noordik JH (2000) J Comput Aided Mol Des 14:123–134
39. Frisch MJ, Trucks GW, Schlegel HB, Scuseria GE, Robb MA, Cheeseman JR, Zakrzewski VG, Montgomery JA, Stratmann RE, Burant JC, Daprrich S, Millam JM, Daniels AD, Kudin KN, Strain MC, Farkas O, Tomasi J, Barone V, Cossi M, Cammi R, Mennucci B, Pomelli C, Adamo C, Clifford S, Ochterski J, Petersson GA, Ayala PY, Cui Q, Morokuma N, Rega N, Salvador P, Dannenberg JJ, Malick DK, Rabuck AD, Raghavachari K, Foresman JB, Cioslowski J, Ortiz JV, Baboul AG, Stefanov BB, Liu G, Liashenko A, Piskorz P, Komaromi I, Gomperts R, Martin RL, Fox DJ, Keith T, Al-Laham MA, Peng CY, Nanayakkara A, Challacombe M, Gill PMW, Johnson BG, Chen W, Wong MW, Andres JL, Gonzalez C, Replogle ES, Binkley JS, Defrees DJ, Baker J, Stewart JP, Head-Gordon M, Pople JA (2001) Gaussian 98, Revision A.11.2. Gaussian Inc., Pittsburgh, PA
40. Cremer D, Pople JA (1975) J Am Chem Soc 97:1354–1358
41. Zefirov NS, Plyulin VA (1980) Dokl Akad Nauk SSSR 252:111–115
42. Haasnoot CAG (1992) J Am Chem Soc 114:882–887
43. Comba P, Remenyi R (2003) Coord Chem Rev 238–239:9–20
44. Jones RO (1991) Angew Chem Int Ed Engl 30:630–640
45. Piela L, Kostrowicki J, Scheraga HA (1989) J Phys Chem 93:3339–3346
46. Honark V, Simmerling C (2003) Proteins: Structure, Function, and Genetics 51:577–590
47. Hornak V, Abel R, Okur A, Strockbine B, Roitberg A, Simmerling CL (2006) Proteins: Struct Funct Bioinform 65:712–725
48. Duan Y, Wu C, Chowdhury S, Lee MC, Xiong G, Zhang W, Yang R, Cieplak P, Luo R, Lee TJ (2003) J Comput Chem 24:1999–2012
49. Jorgensen WL, Chandrasekhar J, Madura JD, Impey RW, Klein ML (1983) J Chem Phys 79:926–935

50. Guimarães CRW, Barreiro G, Augusto C, de Oliveira F, de Alencastro RB (2004) Braz J Phys 34:126–136
51. Case DA, Darden TA, Cheatham TE III, Simmerling CL, Wang J, Duke RE, Luo R, Merz KM, Wang B, Pearlman DA, Crowley M, Brozell S, Tsui V, Gohlke H, Mongan J, Hornak V, Cui G, Beroza P, Schafmeister C, Caldwell JW, Ross WS, Kollman PA (2004) Amber 8. University of California, San Francisco
52. Poteau R, Trinquier G (2005) J Am Chem Soc 127:13875–13889
53. Tuckerman ME, Marx D, Parrinello M (2002) Nature 417:925–929
54. Bizzarri AR, Cannistraro S (2002) J Phys Chem B 106:6617–6633
55. Hartsough DS, Jr Merz KM (1993) J Am Chem Soc 115:6529–6537
56. Berendsen HJC, van Gunsteren WF, Zwinderman HRJ, Geurtsen RG (1986) Ann NY Acad Sci 482:268–286
57. Bizzarri AR, Wang CX, Chen WZ, Cannistraro S (1995) Chem Phys 201:463–472
58. Tirado-Rives J, Jorgensen WL (1990) J Am Chem Soc 112:2773–2781
59. Reddy CK, Das A, Jayaram B (2001) J Mol Biol 314:619–632
60. Mezei M, Beveridge DL (1981) J Chem Phys 74:622–632
61. Stillinger FH, Rahaman A (1974) J Chem Phys 60:1545–1557
62. Balasubramaniam S, Pal S, Bagchi B (2002) Phys Rev Lett 89:115505–1–115505–4
63. Pal S, Balasubramaniam S, Bagchi B (2003) Phys Rev E 67:061502–1–061502–10
64. Bandyopadhyay S, Chakraborty S, Balasubramaniam S, Pal S, Bagchi B (2004) J Phys Chem B 108:12608–12616
65. Bandyopadhyay S, Chakraborty S, Balasubramaniam S, Pal S, Bagchi B (2005) J Am Chem Soc 127:4071–4075
66. Bandyopadhyay S, Chakraborty S, Bagchi B (2005) J Am Chem Soc 127:16660–16667
67. Wider G, Riek R, Wüthrich K (1996) J Am Chem Soc 118:11629–11634
68. Wüthrich K, Billeter M, Güntert P, Luginbühl P, Riek R, Wider G (1996) Faraday Discuss 103:245–253